



FEM Optimisation of Seepage Control System Used for Base Stability of Excavation

Ilyes Ouzaid ^{a*}, Naïma Benmebarek ^a, Sadok Benmebarek ^a

^a Department of Civil and Hydraulic Engineering, NMISSI Laboratory, Biskra University, Algeria.

Received 31 May 2020; Accepted 20 August 2020

Abstract

With the existence of a high groundwater level, the head difference between the inside and outside of an excavation may lead to the loss of stability of the excavation's surface. Hence, a fundamental understanding of this occurrence is important for the design and construction of water-retaining structures. In some cases, the failure mechanism cannot be predicted exactly because of its mechanical complexity as well as a major lack of protection systems and not adopting effective countermeasures against this phenomenon. The article took a tranche from an 80 km long open sewer located in the Ruhr area, Germany as an example to establish a hydro-geological model and analyse the instability of the excavation base surface caused by the groundwater flow at 45m deep and to present the effectivity of an adopted drainage system inside the excavation pit as 39 columns of sand to relax the pore water pressure. By using the Finite Element Method (FEM) analysis, the failure mechanism was investigated before applying any countermeasures, and the total length of the adopted countermeasure system was minimised. Also, various position tests were performed on the adopted drainage system to confirm the optimised position. The results of this numerical study allowed the deduction of the importance of the used drainage system by achieving 44% more in the excavating process. After achieving the required excavation depth, a further increase of the sand columns' penetration may be considered non-economic because, after adding extra depth, all the situations have the same safety factor. In addition, this can provide a reference for the optimised position of the sand columns where they must be applied right by the wall and limited by a critical distance, $D/2$, half of the embedded depth of the wall.

Keywords: Factor of Safety; Failure Mechanism; Deep Circular Excavation; Finite Element Method; Drainage System.

1. Introduction

Deep excavation projects under retaining walls are increasing in recent years along with the growth of infrastructure needs and the development of urban sites for basements and tunnels. The limitation on open lands for further development is one of the reasons behind that trend. When the depth of a planned excavation pit is lower than the groundwater level in the field, the groundwater head difference between the inside and outside leads to basal failure of the excavation pit. In some cases, the failure mechanism cannot be predicted precisely because of its mechanical complexity, and it is extremely difficult to stop these phenomena once they start, as well as a notable lack of both protection systems and adoption of effective countermeasures against this phenomenon. In the design of deep excavation under conditions with a high groundwater level, several issues are related to the stability of the excavation. These are often dominated by the water flow around the wall and include upheaval failure, general shear failure and sand boiling failure [1].

* Corresponding author: ouzaid.ilyes@univ-biskra.dz

 <http://dx.doi.org/10.28991/cej-2020-03091579>



© 2020 by the authors. Licensee C.E.J, Tehran, Iran. This article is an open access article distributed under the terms and conditions of the Creative Commons Attribution (CC-BY) license (<http://creativecommons.org/licenses/by/4.0/>).

Therefore, for a clearer understanding of the basal failure phenomenon of the excavation pit and its mechanisms, various methods (theoretical, numerical and experimental) have been addressed in literature and reported in this work.

According to EN 1997-1/Eurocode 7 [2], heave, uplift, internal erosion or piping represents the failure mechanisms induced by seepage flow. Heave appears when the seepage forces developed by groundwater flow lift the soil on the downstream side. Also, when seepage forces are acting on the subsoil, especially the upward seepage close to the excavation level, where the seepage forces could be higher than the effective weight of the soil, failure by uplift occurs. Along with seepage, internal erosion or piping might occur with the transport of soil grains within a soil layer at the interaction surface of a soil layer and a structure by groundwater flow, or starting with a pipe-shaped canal on the downstream side and propagating backwards, respectively, which may finally lead to collapse, as shown in Figure 1.

The most used verification method was presented by Terzaghi (1943) [3]. He used model tests to study the influence of seepage flow on the stability of retaining excavations. He found that a rectangular prism, adjacent to the wall, could be assumed to be the failure shape lifted by pore water pressure. The total height of the rectangular prism corresponds to the embedment depth of the wall from the surface of the excavation pit to the toe of the excavation wall, and its width is half of the embedded depth of the wall. Experimental tests on the sand model were examined by Tanaka and Verruijt (1999) [4] to describe the mechanism of basal failure of the excavations. They found that the critical hydraulic head differences discovered by Terzaghi and prismatic failure are close to the head difference at the start of deformation. Based on the experimental results of twelve centrifugal model tests, Sun (2016) [5] presented two types of failure: general upheaval and local failure (sand piping and sand boiling). He compared the experimental results with calculated results obtained from the developed approach to the stability analysis of deep excavation against a confined aquifer. The results showed good agreement.

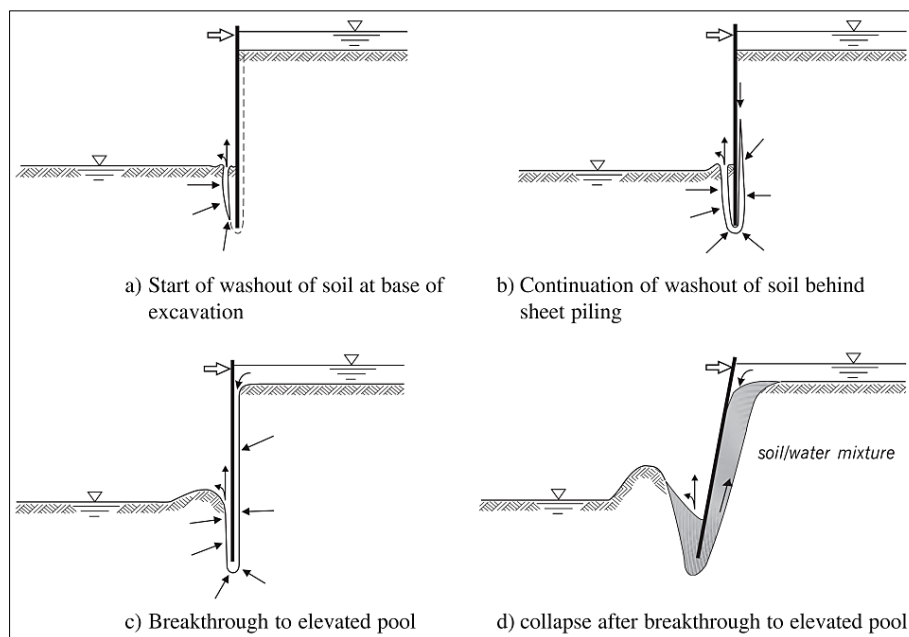


Figure 1. The development of piping around waterfront structures according to EAU (2004)

Considering a fixed wall, which may represent a sheet pile strut, Benmebarek et al. (2005) [6] used the explicit finite difference method FLAC 2D code to analyse the failure of sandy soil within a cofferdam subjected to an upward seepage flow. Their results identified different failure mechanisms at the downstream side occurring for critical hydraulic head loss, which were greatly influenced by the interface and soil characteristics. Benmebarek et al. (2014) [7] investigated the critical height of water on the upstream side of free and fixed sheet pile walls using the commercial code FLAC. They found that seepage failure by basal heaving given by Terzaghi's discovery is less critical than the obtained rotational failure. Aulbach and Ziegler (2013) [8] numerically analysed the excavation stability of steady-state flow and presented a triangular prism of failure, its height and width being equal to the embedment depth of the wall and its half, respectively.

To study the base stabilities of retaining excavations against seepage failure by heave where a relatively permeable cohesionless soil layer lies above a less permeable soil layer between the excavation base and wall toe, Koltuk et al. (2019) [9] compared the results of numerical simulations and experimental tests with those obtained from Terzaghi and Peck's approach. Both the numerical analysis and the model tests showed a good agreement in which a triangle-shaped heave zone with a larger width was obtained, unlike the rectangular-shaped heave zone suggested by Terzaghi and Peck.

The method of fragments was validated by Madanayaka and Sivakugan (2019) [10] to estimate the exit hydraulic gradient and flow rate of axisymmetric circular cofferdams for numerical and experimental models. The results that were determined for both exit hydraulic gradient and flow rate showed an excellent agreement between the numerical model results and experimental results, in which the numerical predictions were within $\pm 5\%$ of the corresponding experimental results. Koltuk and Azzam (2019) [11] performed numerical analyses and experimental tests of quicksand conditions in cohesionless soils to estimate the base stability of a retained excavation against seepage failure by heave. The results showed that the potential differences that led to failure were higher than the potential differences that were required for the theoretical approaches and the development of quicksand conditions was unachievable for the situation where a high permeable cohesionless soil layer was overlying a less permeable soil layer between the excavation base and wall tip.

Marsland (1953) [12] studied the mechanisms of failure using sand–water models. He found that the pit dimensions and soil conditions have a clear influence on the hydraulic failure of the excavation pit. For homogeneous soil conditions, the stability increases with increasing the embedment depth of the retaining wall below the excavation base and decreases as the excavation become narrower. Aulbach et al. (2013) [13] generated eight design charts, taking into consideration the geometrical boundary conditions, in order to determine the required embedded length of the excavation retaining system for safety against hydraulic heave. Their results showed clearly that the width has an enormous influence on safety. Faheem et al. (2003) [14] used the finite element method (FEM) to evaluate the two-dimensional base stability of excavations. They stated that the thickness of the soft soil layer between the excavation base and hard stratum, the ratio of the depth to the width of the excavations, the penetration depth of the wall below the excavation base and its stiffness all have a significant influence on the base stability of excavations. Zhang and Goh (2016) [15] used the two-dimensional FEM with shear strength reduction using the commercial software Plaxis 2011 to analysis the basal heave stability of deep narrow braced excavations in terms of stability number and factor of safety. The results indicate that the stability number is independent of undrained shear strength and the system stiffness has a small influence on the factor of safety against basal heave.

A series of parametric studies were carried out by Pratama and Ou (2018) [16] using numerical analysis and the conventional method of flow net to identify the factor of safety values representing the safety against sand boiling and predict the failure mechanism caused by groundwater flow. The results show that the critical width of the soil prism presented by Terzaghi is bigger than that set by the author; likewise, the soil density and excavation geometry has some significant effects in governing the failure mechanism and the hydraulic gradient. To assess the coefficient of security against heaving and investigate the critical heads for the failure of hydraulic structures, Fontana (2008) [17] analysed different thickness sheet piles embedded in sandy soils. Theoretical values and experimental data were compared, showing good agreement if the ground surface deformation and the thickness of the sheet pile are properly taken into account.

Based on the experimental results of Yousefi et al. (2016) [18], where they simulated the seepage flow and its behaviour downstream of a sheet pile under inclined and vertical configurations using laboratory models to study the boiling phenomenon, an inclined configuration with an angle of 60° to the horizontal direction and a ratio of sheet pile depths $d/D=0.34$ and $d/D=0.44$, in which d is the vertical penetration depth of the sheet pile and D is the thickness of the foundation material for inclined and vertical configurations respectively, have successfully reduced the boiling phenomenon and exit vertical hydraulic gradient. Zhao et al. (2020) [19] conducted both an FEM and full-scale in-situ tests in Guangzhou, China, to study the effects of circular shaft diameters on failure by uplift and to analyse its failure mechanisms, as well as to determine a reasonable stability judgement method for circular shafts subjected to hydraulic uplift. The authors found that the observed phenomena on-site have good agreement with the results obtained from the finite element analysis. Pane et al. (2017) [20] presented a methodology based on the simple concept of increasing the drainage capacity of the embedded portion of the retaining walls aimed at minimising the risk of uplift and heave failures of retained excavations. They found that the draining wall can greatly improve heave safety, and the dominant failure mechanism changes from heave to uplift.

From all of the above, it can be seen that most of what has been done in literature did not take place in real excavations, and also focussed just on the analysis aspect without adopting effective countermeasures and providing new techniques for protecting excavation pits against basal failure. In this context, the present paper took a tranche from an 80 km long open sewer located in the Ruhr area, Germany (Figure 4) as an example to establish a hydro geological model and analyse the instability of the excavation base surface caused by the groundwater flow using the powerful geotechnical software, Plaxis v. (2012). The maximum achieved depth of the excavation and the failure mechanism before applying the drainage system was checked out and compared with previous research. As a next step, this study presented the affectivity of the adopted drainage system inside the excavation pit to relax the pore water pressure in order to achieve the required excavation depth. Finally, it optimised the length of the adopted drainage system and studied its position effect from the wall, taking into consideration the economic and safety aspects. The following flowchart (Figure 2) presents the methodology employed in this study.

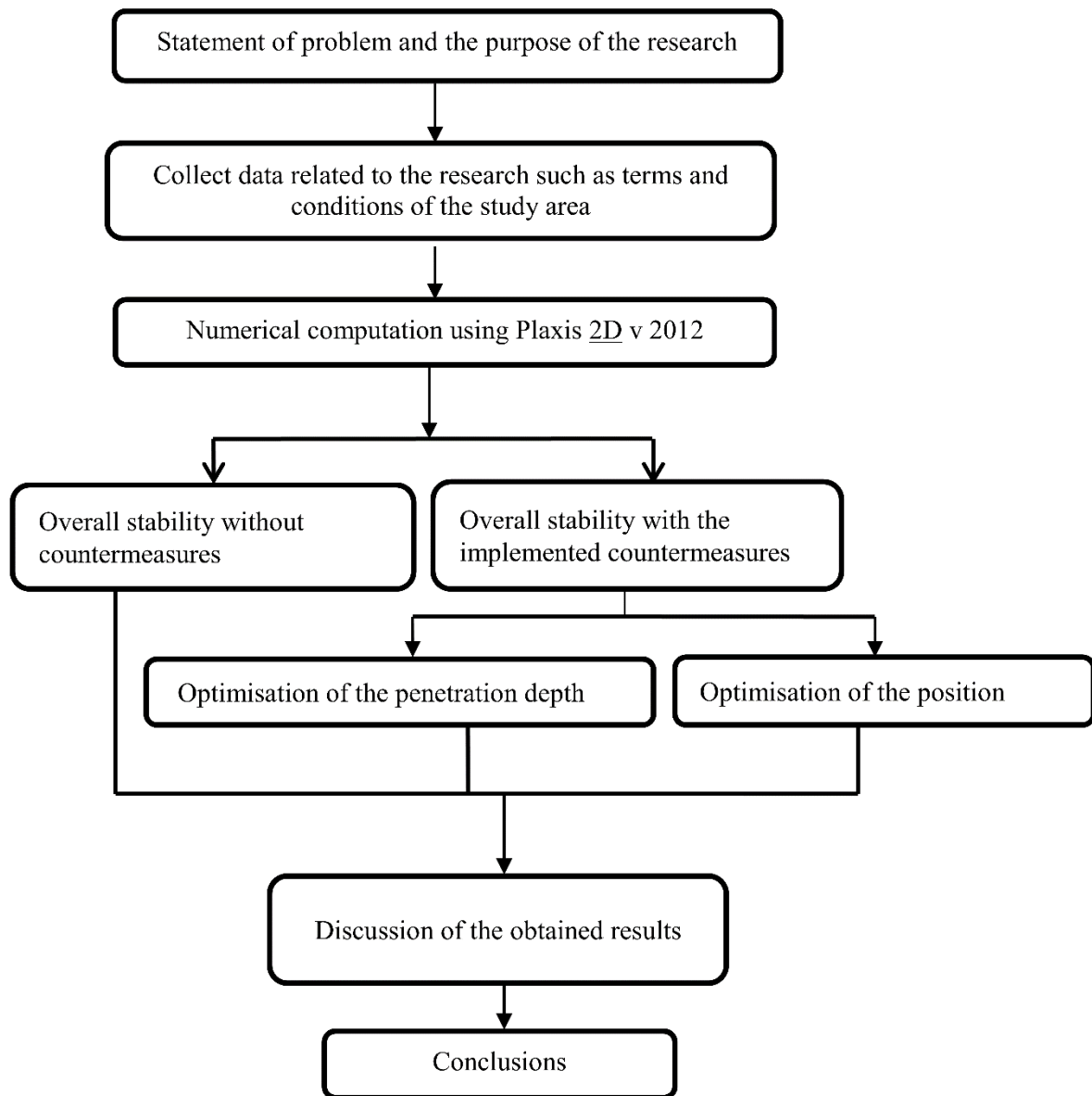


Figure 2. Research methodology flow chart

2. Case Study

Since the period of industrialisation, wastewater in the Ruhrgebiet in Germany has drained into the east–west river of Emscher. Now, due to the world’s most modern sewage system, the river of Emscher will be converted into a near-natural body of water in order to restore the natural condition of the Emscher and its tributaries. The overall project is over a length of 51 km, between Dortmund-Deusen and the mouth of the Emscher in Dinslaken, where the wastewater will flow in closed piped channels of about 400 km of sewer tunnels with a maximum outside diameter of 4.20 metres that are up to 40 m deep.

In the area of section 40 (Figures 3 and 4), data from laboratory investigations have been collected where 300 boreholes were drilled to a depth of about 70 m in order to investigate the soil characteristics. The information gained mostly showed that the site consists of two main layers, Quaternary sand, predominantly with underlying cohesive soils such as marl. Figure 5 shows the schematics of the systematised geotechnical longitudinal section of construction section 40.



Figure 3. The main course of the Emscher

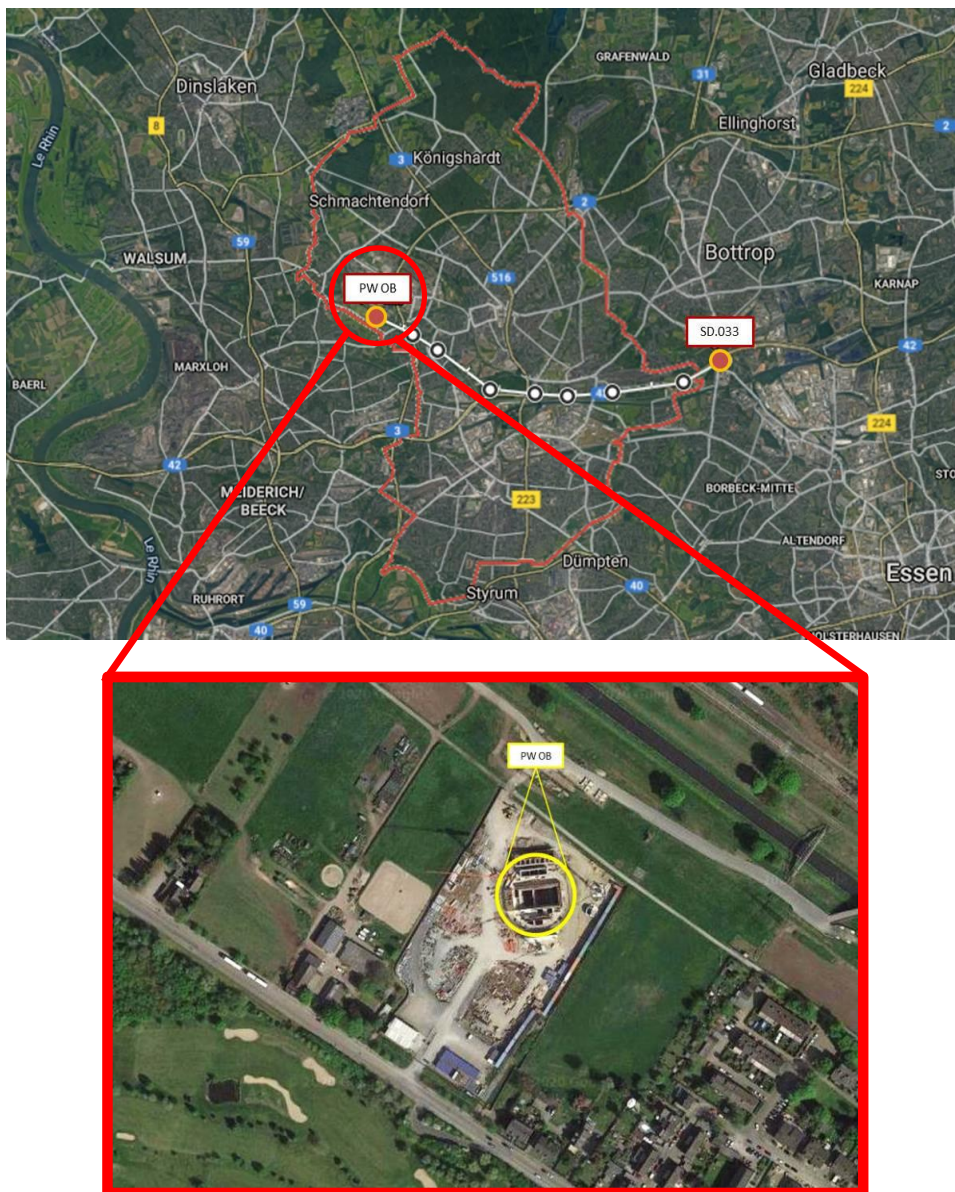


Figure 4. The site of the study area in section 40

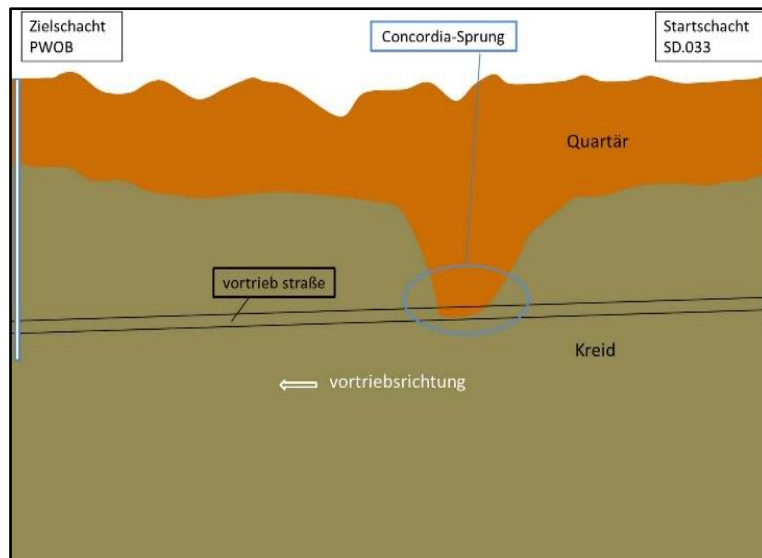


Figure 5. The systematised, geotechnical longitudinal section of construction section 40

Figure 6 shows the grain size range of the Cretaceous ground (solid lines) passed through in the west half of section 40 and the grading distribution of the material of the Concordia-Sprung in the east half of section 40 (dashed lines).

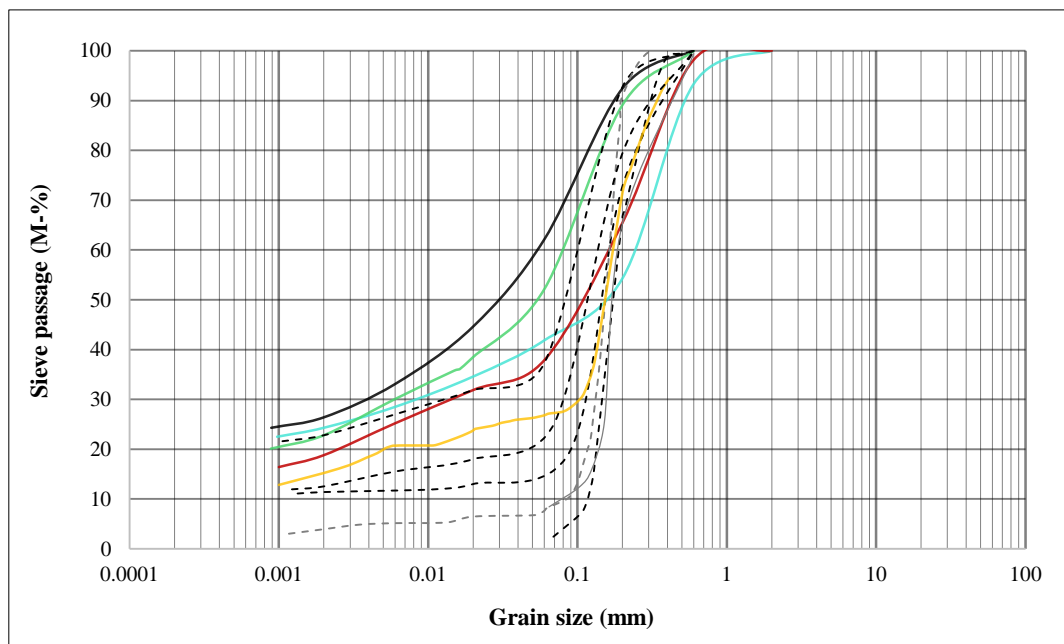


Figure 6. Typical grading curves in the Cretaceous determined in the site investigation (solid lines) and typical grading curves in the Concordia-Sprung fault zone (dashed lines)

Various types of marl can be distinguished along the route of construction section 40 (Route of the Interceptor SD.033 - PW OB). The Emscher marl is the predominant deposit and consists of glauconitic, calcareous, clayey silts and calcareous silty fine sands, which are consolidated to clay or sand marl and clay or calcareous marlstone. Above the Emscher marl are the Osterfeld beds, which consist of marly and silty fine sands, mostly with a considerable medium sand content, as well as very sandy silts. The Bottrop beds, which partly overlie the Osterfeld beds, consist of grey-green glauconitic fine sand marlstone, which transitions at the base from marly fine to medium sands. The upper part of the Bottrop beds consists of marlstones and fine sandy clay marlstones. At its surface, the marl is mostly softened and weathered. The Cretaceous beds dip flatly to the north-northwest. Additional tectonic faults lead to all these Cretaceous strata being passed through by the tunnel drive.

In this paper, the western half of section 40 (PW OB) was taken as a case study, where the Emscher marl is the predominant deposit, falling under mostly a considerable medium sand.

3. Numerical Simulation of the Case Study

In both cases – cohesive soil and groundwater relaxing system – the classical method fails. Here, numerical simulations based on the FEM appear to be a helpful tool, since they present the relevant failure mechanism as a result of the calculation. The FE modelling method using the Plaxis 2D- V 2012 computer program has been applied to the case study of a deep excavation PW-OB located in section 40 (Figure 4). Using the numerical method advantages, an axisymmetric model is used where the FE mesh consists of 15-nodes of triangular elements. The size of the calculation model was chosen so that the boundaries do not influence the deformation behaviour of the model. Theoretically, the tensile stresses that can be absorbed by the ground are cut-off. In order to simulate the excavation and construction process as a real case, the calculation was divided into several steps based on the actual excavation planning. According to the data of the previous on-site investigation and the laboratory tests, the parameters, such as the permeability, the modulus and so on, for every soil are determined with the Mohr-Coulomb model used for all soil layers. The soil parameters for the simulation are summarised in Table 1.

Table 1. Main hydraulic and mechanical properties of the soils

Parameter	Quaternary sand	Marl	Clean Sand
Unsaturated unit weight γ_{unsat} (kN/m ³)	19	20	19
Saturated unit weight γ_{sat} (kN/m ³)	20	22	20
Friction angle (°)	30	25	30
Cohesion (kN /m ²)	0	40	0
Dilation angle (°)	0	0	0
Poisson's ratio	0.3	0.25	0.33
Wall-friction and -adhesion R	0.5	0.2	1
Permeability (m/s)	1×10^{-4}	1×10^{-6}	1×10^{-3}
Young's modulus (kN /m ²)	29,700	40,000	20,200

Figure 7 presents the project where the case study was chosen for this paper. It shows a circular excavation with an inside diameter $B=46$ m and a depth $d=45$ m, as the three-dimensional model presented in Figure 8. The surrounding soil is retained by an impermeable wall of 2 m in thickness. The wall is inserted by $D=6$ m beneath the final excavation.



Figure 7. Presentation of the pit chosen for this paper (PWOB)

To relax the pore water pressure that causes excavation bottom instability due to the different groundwater level where the outside level is higher than inside the excavation, 39 clean sand columns with a diameter of 30 cm reaching down to a depth of $t_e = 90$ m from the ground surface, and 2m away from the wall were modelled as a concentric thin slot. Sandy columns with relatively high permeability ($k=10^{-3}$ m/s) are an appropriate measure to improve the hydraulic situation at the bottom of the excavation. For the initial state, the groundwater was set at 6 m below the top of the site.

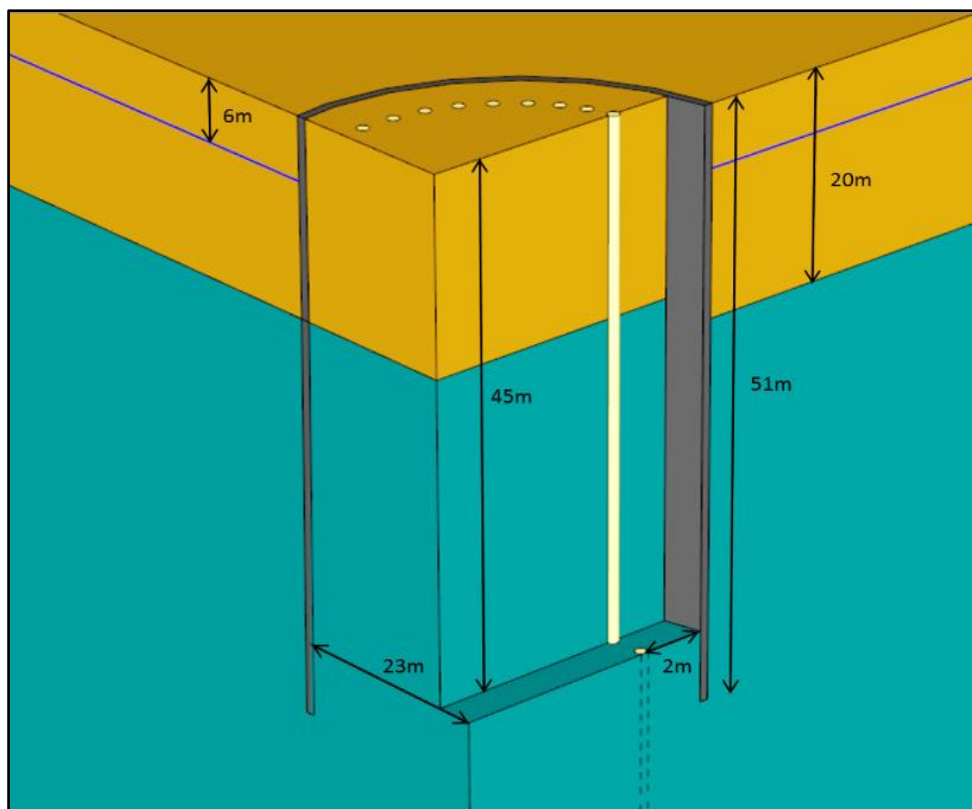


Figure 8. Three-dimensional model of relatively wide circular-shaped excavation pit

The mathematical modelling of the groundwater flow resulting from the excavation of the soil and simultaneous drainage via the retaining wall and the bottom of the construction pit is based on Darcy's law. The effective stress was calculated in the form of a coupled analysis, i.e. the distribution of the pore water pressure determined in a calculation of flow and used as the initial condition for the subsequent stress calculation. The groundwater flow calculated in the respective excavation state and the calculated flow pressure describes the steady-state.

4. Results and Discussion

4.1. Overall Stability without Countermeasures

The following investigation deals with the verification against excavation bottom instability. The first part of this research work consists of evaluating the maximum excavation depth that can be reached without applying any countermeasures.

After calculating the initial stress state by initialising the stresses in the model with the coefficient K_0 of lateral pressure of the earth at rest $K_0 = 1 - \sin\phi$, the excavation states were displayed in 1 m excavation steps and here the calculation of the strain state under stress was coupled to the calculation of the groundwater flow.

The performed calculations indicate that the excavation process is safe enough without any countermeasures reaching down to a depth of 25 m from the ground surface. For a deeper excavation process, the situation would be exposed to the collapse of the excavation base. Here, the drainage system (sand columns) must be installed. In order to demonstrate the failure mechanism, the drilling process was attended up to 26 m, where the bottom of the excavation at that depth was affected by hydraulic failure.

Figure 9 shows the path of the groundwater within the soil of the studied case at the critical moment where the excavation base is exposed to collapse. The water located in the upper layer goes in a horizontal direction and accumulates at the wall front, then fast-flowing down creates an intensive upward seepage force at the downstream side. The reason for this is that the low permeability of the lower layer (marl) creates isolation at the soil interface leading to preventing water from passing down on the ground.

At the moment where the situation exposed to the collapse of the excavation base, Figure 10 shows the mechanism of failure. The soil at the base of the excavation lifted completely owing to the intensive upward seepage forces resulting from the ground stratification and their different soil permeability. It appears as general heave, and the prism of failure does not give a specific region.

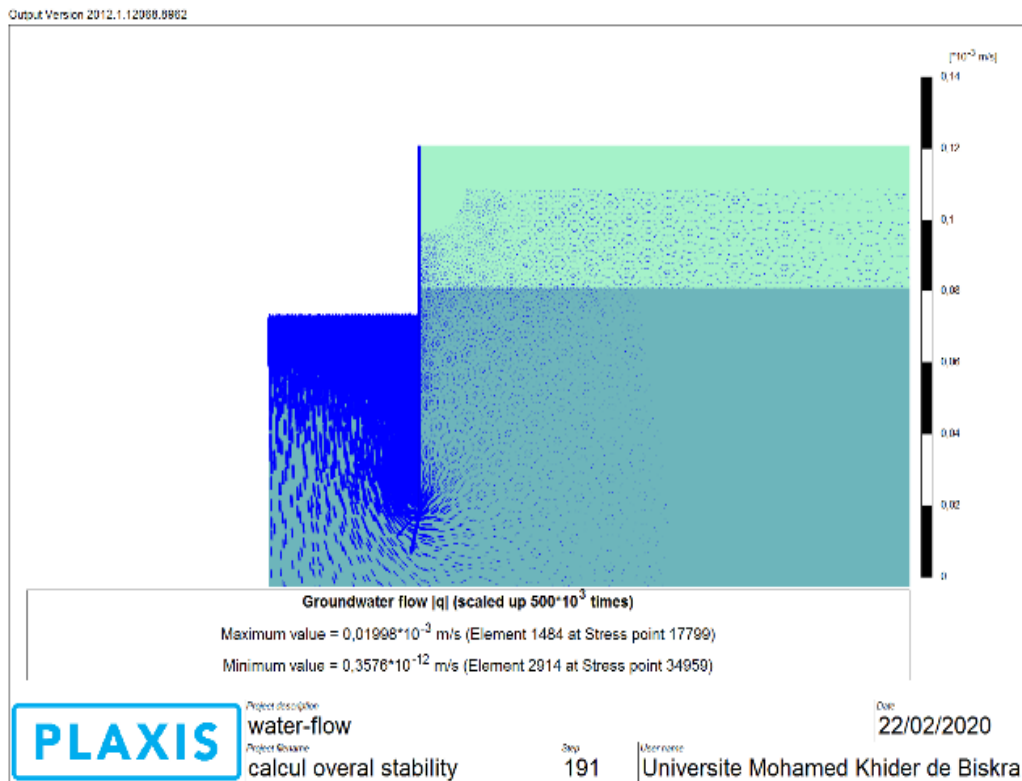


Figure 9. The path of the groundwater flow through the soil

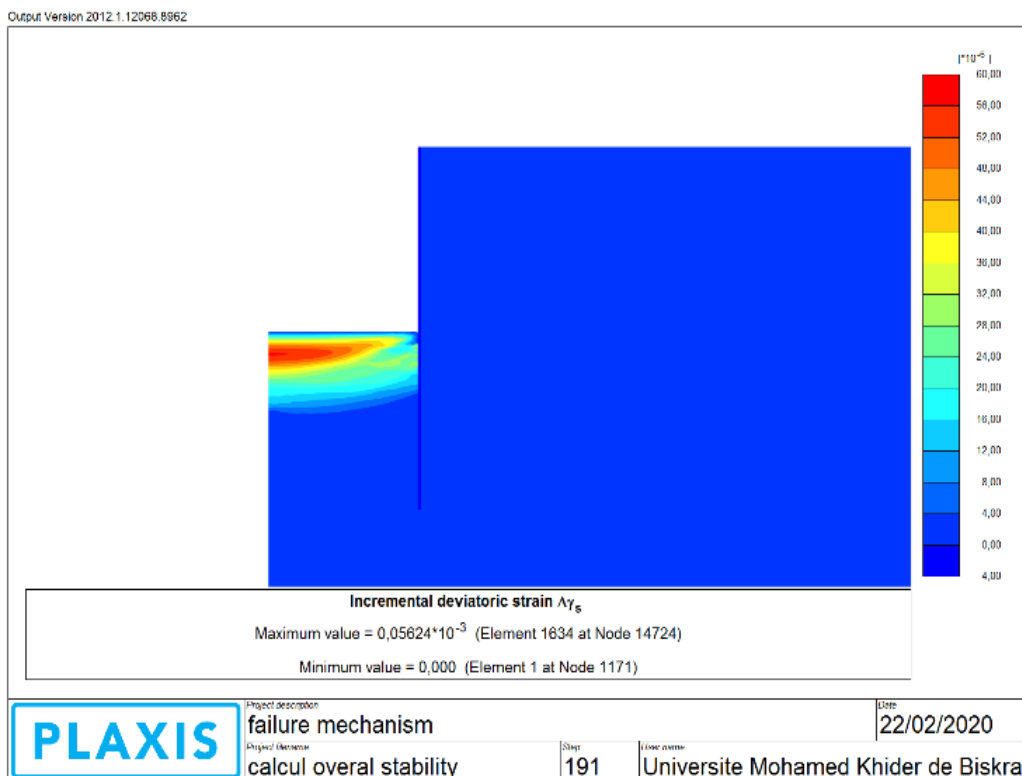


Figure 10. The capture of failure mechanisms before applying the countermeasures

Comparing the obtained failure mechanism from this study to those accomplished by Benmebarek et al. (2005 and 2014), Aulbach and Ziegler (2013) and Koltuk et al. (2019) [6-9] in which three types of failure have been presented (triangular, rectangular prisms and boiling) and the rectangular failure body with width $D/2$ represented by Terzaghi (1943) [3], shows clearly that they are not in good agreement. Therefore, it becomes clear that for real cases, where horizontal stratification exists between the excavation base and the wall tip and for specific soil characteristics, the mechanism of failure cannot be generalised to all situations, and its diagnosis varies from case to case.

4.2. Overall Stability with the Implemented Countermeasures

As countermeasures, the second part of this research is related to applying the drainage system and testing its effectivity against the failure of the excavation base due to the water seepage forces. For this project, the implemented drainage system consists of 39 columns of sand with a high coefficient of permeability reaching down 90 m from the ground surface. As the material of the drainage system consists of sand, the 39 clean sand columns can easily be excavated with the surrounding soil.

The results indicate that, for all the excavation states, the situations have the required safety to achieve the targeted depth of 45 m deep and the drainage system is very effective to absorb the seepage forces. However, it is not clear which failure mechanism becomes relevant in the case of excavations with a drainage system in the subsoil. It does not seem to be admissible to transfer the classical failure mechanisms to these situations.

In aiming to give the present case study more precise design values in economic terms, and taking into consideration safety as the first criterion, varied depths and positions of the drainage system have been analysed.

4.3. Optimisation of the Penetration Depth

In order to study the effect of the drainage system penetration beneath the subsoil, the length of the columns, t_e , is reduced from the designed value, 90 m, by a step of 3.5 m, while keeping the same characteristics of the soils, until the occurrence of collapse at the base of the excavation. The results presented in Figure 11 indicate that for a penetration depth of 76 m of the drainage system beneath the subsoil, the geo-hydraulic situation is safe enough against the failure of the excavation base. At a further reduction in the penetration depth of the drainage system (less than 76 m), the situation falls, and collapse occurs. From a depth of penetration of 76 m to 83 m the safety factor (FS) went up slightly, taking the value from 1.1624 to 1.1647; however, it remained stable from 86.5 m to 90 m. That slight increase of FS value may be considered non-economic because, at a depth of penetration of 76 m, all the excavation states have the required safety. The reason for this could be that the flow path from upstream was limited by global driving contours, whereas the point of intersection for the lower limit of this with the drainage system was located at -76 m from the ground's surface. The other deepest flow path can be considered non-influential on the behaviour of the phenomenon.

Also, the permeability of the drainage material has been reduced in order to test its effect on the stability of the excavation base. The results indicate that for permeability of less than $k < 10^{-3}$ (m/s), the seepage problem cannot be resolved no matter how deep the drainage system is.

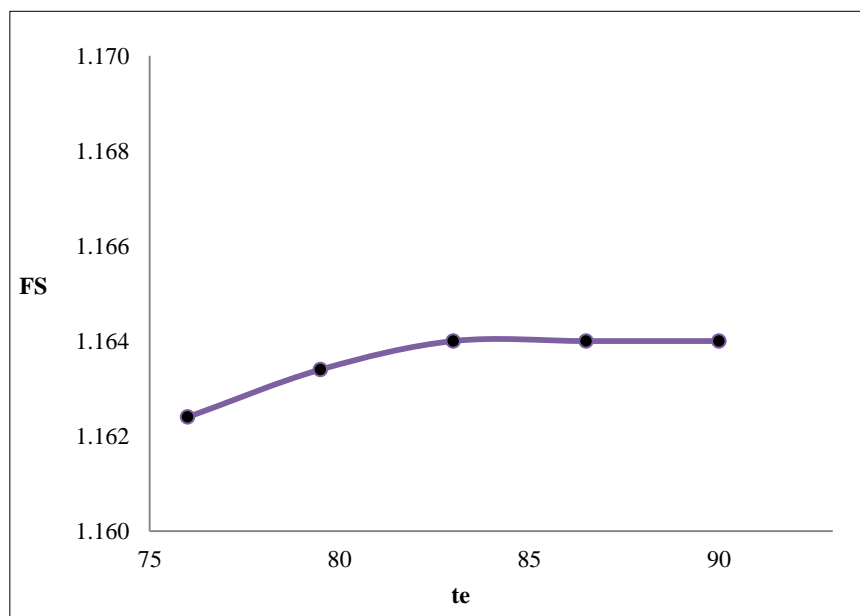


Figure 11. Effect of drainage system penetration

4.4. Optimisation of the Position

In this part, the drainage system moved from the wall going to the centre of the pit with a distance d_e by a step of 0.5 m. The first position was attached to the wall with a distance of 0.25 m, as it is the nearest possible position to the wall. In each step, the factor of safety has to be gained for each position ending at the optimal position.

Figure 12 shows that from position $D/2$ of the drainage system closer to the wall, the factor of safety is raised and achieves the maximum value near the wall. In other words, from the other side with the position $D/2$ of the drainage system heading towards the middle of the pit, the process of the excavations fails before achieving the required depth (45 m deep) and the drainage system cannot solve the situation even if reaches very deep. Here, it could be noted that, for the analysis of the basal heave of excavations, the upward seepage flow from the upstream side is limited by the diving contours with a distance $D/2$ from the wall.

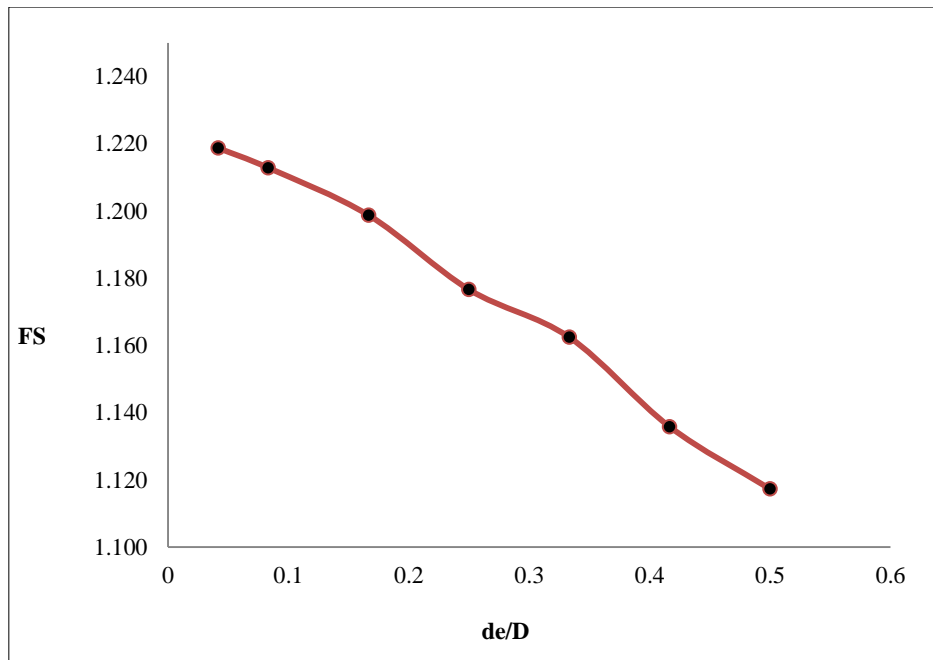


Figure 12. Effect of drainage system position

Comparing what was mentioned in the literature by Terzaghi (1943) [3], where the relevant zone suggested for seepage failure is a rectangular prism adjacent to the wall with $D/2$ in width (Figure 13), with the acceptable limit of drain positions developed from this study, they are obviously in good agreement. Lastly, through the obtained results, it could be supposed that for the stability of the excavation base against seepage flow, the mechanism of failure is not related to the vulnerable region.

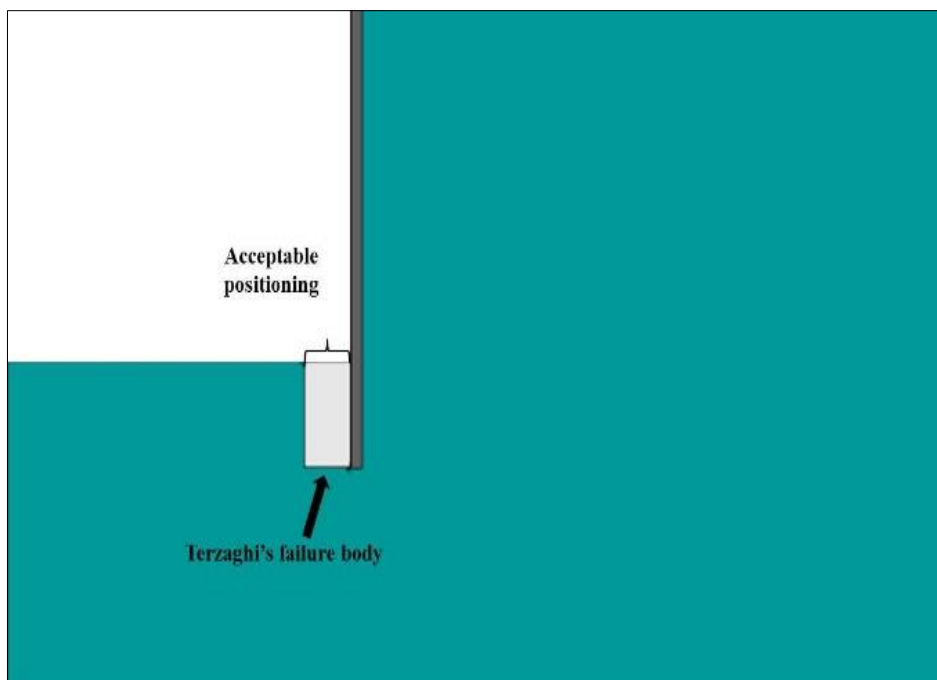


Figure 13. The acceptable positioning of the drainage system

5. Conclusions

Safety against water flow in deep excavations represents a crucial aspect of design. In many cases, both the design and the overall cost of the excavation system are dictated by this problem of hydraulic failure. In this research, a real project of deep-braced excavation located in the Ruhrgebiet, Germany, subjected to seepage flow, was established using the elastic–plastic FEM to predict the failure mechanism caused by groundwater flow and to perceive the factor of safety values against the failure of the excavation base. A drainage system, consisting of clean sand with high permeability, was adopted and implemented for this case study to relax the excess pore water pressure. This has been numerically tested for its effectivity. To underscore the scientific value of this research work, the optimised length of the drainage system and its effective position from the wall have been analysed with regard to the economic aspect, bearing in mind safety as the first criterion. The results that have been mentioned in the literature were compared with those obtained by numerical simulations in this work. The conclusions are as follows:

- Before applying any countermeasures, the soil at the base of the excavation lifted completely owing to the intensive upward seepage forces resulting from the ground stratification and their different soil permeability. In that situation, the achieved excavation depth was slightly more than half of the required depth. The mechanism of failure appears as general heave, and the prism of failure does not give a specific region. Therefore, it becomes clear that for real cases, where horizontal stratification exists between the excavation base and the wall tip and for specific soil characteristics, the mechanisms of failure cannot be generalised to all situations, and their diagnosis varies from case to case.
- To achieve the required excavation depth, the adopted drainage system has been implemented. Results showed that the drainage system was quite an effective countermeasure against the failure of the excavation base.
- By analysing the effect of the drainage system penetration beneath the subsoil, results indicated that with 76 m in penetration depth, the drainage system could sufficiently support the geo-hydraulic situation against the failure of the excavation base. A slight increase in the safety factor when the drainage system reached down 90 m, however, may be considered a non-economic decision.
- From the position $D/2$ of the drainage system going closer to the wall, all excavation processes were safe enough until reaching the required depth and the factor of safety was raised and achieved the maximum value near the wall. Otherwise, the drainage system could not resolve the situation even if they reached very deep, and the process of the excavation failed before achieving the required depth.
- For similar projects subjected to hydraulic heave, the obtained results can be provided as a reference to use for stability evaluation with regards to the applicability of the adopted system and its efficacy of safety and economy.

5.1. Future Aspects of the Research

The overall performance of the drainage system, which consists of clean sand, to be reported as satisfactory. More research must be carried out in order to determine the possible effective countermeasures against a basal failure of excavation. The authors suggest treating the problems using the technique of stone columns with the installation effect for which it has the best correlation regarding the drainage and improvement of its surrounding soil.

6. Acknowledgements

The authors express their gratitude to the Directorate General for Scientific Research and Technological Development of Algeria. They also gratefully acknowledge the support from the Department of Geotechnical Engineering of Duisburg-Essen University, Essen, Germany for providing the opportunity to do this research work and making the various resources available.

7. Conflicts of Interest

The authors declare no conflict of interest.

8. References

- [1] Ou, Chang-Yu. “Deep Excavation” (April 21, 2014). doi:10.1201/9781482288469.
- [2] “Eurocode 7. Geotechnical Design” (2004). doi:10.3403/03181153u.
- [3] Terzaghi, Karl. “Theoretical Soil Mechanics. Johnwiley & Sons.” New York (1943): 11–15.
- [4] Tanaka, Tsutomu, and Arnold Verruijt. “Seepage Failure of Sand behind Sheet Piles—The Mechanism and Practical Approach to Analyse —.” *Soils and Foundations* 39, no. 3 (June 1999): 27–35. doi:10.3208/sandf.39.3_27.

- [5] Sun, Yu-yong. "Experimental and Theoretical Investigation on the Stability of Deep Excavations against Confined Aquifers in Shanghai, China." *KSCE Journal of Civil Engineering* 20, no. 7 (January 22, 2016): 2746–2754. doi:10.1007/s12205-016-0488-3.
- [6] Benmebarek, N., S. Benmebarek, and R. Kastner. "Numerical Studies of Seepage Failure of Sand within a Cofferdam." *Computers and Geotechnics* 32, no. 4 (June 2005): 264–273. doi:10.1016/j.compgeo.2005.03.001.
- [7] Benmebarek, N., A. Bensmaïne, S. Benmebarek, and L. Belouar. "Critical Hydraulic Head Loss Inducing Failure of a Cofferdam Embedded in Horizontal Sandy Ground." *Soil Mechanics and Foundation Engineering* 51, no. 4 (September 2014): 173–180. doi:10.1007/s11204-014-9274-8.
- [8] Aulbach, Benjamin, and Martin Ziegler. "Simplified Design of Excavation Support and Shafts for Safety against Hydraulic Heave / Einfache Bemessung von Baugruben Und Schächten Im Hinblick Auf Die Sicherheit Gegen Hydraulischen Grundbruch." *Geomechanics and Tunneling* 6, no. 4 (August 2013): 362–374. doi:10.1002/geot.201300031.
- [9] Koltuk, Serdar, Jie Song, Recep Iyisan, and Rafiq Azzam. "Seepage Failure by Heave in Sheeted Excavation Pits Constructed in Stratified Cohesionless Soils." *Frontiers of Structural and Civil Engineering* 13, no. 6 (September 27, 2019): 1415–1431. doi:10.1007/s11709-019-0565-z.
- [10] Madanayaka, Thushara Asela, and Nagaratnam Sivakugan. "Validity of the Method of Fragments for Seepage Analysis in Circular Cofferdams." *Geotechnical and Geological Engineering* 38, no. 2 (October 31, 2019): 1547–1565. doi:10.1007/s10706-019-01111-9.
- [11] Koltuk, Serdar, and Rafiq Azzam. "Use of Quicksand Condition to Assess the Base Stabilities of Sheeted Excavation Pits Against Seepage Failure in Cohesionless Soils." *Arabian Journal for Science and Engineering* 44, no. 10 (May 2, 2019): 8515–8526. doi:10.1007/s13369-019-03890-y.
- [12] Marsland, Arthur. "Model Experiments to Study the Influence of Seepage on the Stability of a Sheeted Excavation in Sand." *Géotechnique* 3, no. 6 (June 1953): 223–241. doi:10.1680/geot.1953.3.6.223.
- [13] Aulbach, Benjamin, Martin Ziegler, and Holger Schüttrumpf. "Design Aid for the Verification of Resistance to Failure by Hydraulic Heave." *Procedia Engineering* 57 (2013): 113–119. doi:10.1016/j.proeng.2013.04.017.
- [14] Faheem, Hamdy, Fei Cai, Keizo Ugai, and Toshiyuki Hagiwara. "Two-Dimensional Base Stability of Excavations in Soft Soils Using FEM." *Computers and Geotechnics* 30, no. 2 (March 2003): 141–163. doi:10.1016/s0266-352x(02)00061-7.
- [15] Zhang, Fan, and Anthony T. C. Goh. "Finite Element Analysis of Basal Heave Stability for Braced Excavations in Clays." *Japanese Geotechnical Society Special Publication* 2, no. 44 (2016): 1551–1554. doi:10.3208/jgssp.atc6-03.
- [16] Pratama, Ignatius Tommy, and Chang-Yu Ou. "Analysis of Sand Boiling Failure in Deep Excavations." *Proceedings of the 2nd International Symposium on Asia Urban GeoEngineering* (2018): 125–141. doi:10.1007/978-981-10-6632-0_10.
- [17] Fontana, Nicola. "Experimental Analysis of Heaving Phenomena in Sandy Soils." *Journal of Hydraulic Engineering* 134, no. 6 (June 2008): 794–799. doi:10.1061/(asce)0733-9429(2008)134:6(794).
- [18] Yousefi, Mehdi, Mohammad Sedghi-Asl, and Mansour Parvizi. "Seepage and Boiling Around a Sheet Pile under Different Experimental Configuration." *Journal of Hydrologic Engineering* 21, no. 12 (December 2016): 06016015. doi:10.1061/(asce)he.1943-5584.0001449.
- [19] Zhao, Guo-qing, Yu-you Yang, and Su-yun Meng. "Failure of Circular Shaft Subjected to Hydraulic Uplift: Field and Numerical Investigation." *Journal of Central South University* 27, no. 1 (January 2020): 256–266. doi:10.1007/s11771-020-4293-2.
- [20] Pane, Vincenzo, Diego Bellavita, Manuela Cecconi, and Alessia Vecchietti. "Hydraulic Failure of Diaphragm Walls: a Possible Methodology for Safety Improvement." *Geotechnical and Geological Engineering* 35, no. 2 (December 27, 2016): 765–780. doi:10.1007/s10706-016-0140-5.